2023

Comparative Simulations of an Electrochromic Glazing and a Roller Blind as Controlled by Seven Different Algorithms

Hani Alkhatib
Technological University Dublin, Ireland, hani.alkhatib@tudublin.ie

Philippe Lemarchand
Technological University Dublin, philippe.lemarchand@tudublin.ie

Brian Norton
Technological University Dublin, brian.norton@tierc.ie

See next page for additional authors

Funder: This research was funded by MaREI, the SFI Research Centre for Energy, Climate, and Marine [Grant No: 12/RC/2302_P2].

Results in Engineering 20 (2023) 101467

Contents lists available at ScienceDirect

Results in Engineering

journal homepage: www.sciencedirect.com/journal/results-in-engineering

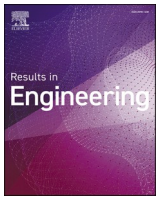

Comparative simulations of an electrochromic glazing and a roller blind as controlled by seven different algorithms

H. Alkhatib [a,b,c,*], P. Lemarchand [a,b,c], B. Norton [a,b,c,e], D.T.J. O'Sullivan [c,d]

[a] School of Electrical and Electronic Engineering, Technological University Dublin, Ireland
[b] Dublin Energy Lab, Technological University Dublin, Dublin, Ireland
[c] MaREI, the SFI Centre for Energy, Climate and Marine, Ireland
[d] IERG, School of Engineering, University College Cork, Cork, Ireland
[e] IERC, International Energy Research Centre, Tyndall National Institute, University College Cork, Cork, Ireland

ARTICLE INFO

Keywords:
Adaptive façade
Building energy efficiency
Electrochromic glazing
Roller blind
Occupancy comfort

ABSTRACT

The use of roller blind as a surrogate for a switchable glazing in a dynamic building environmental simulation is investigated. Seven different control algorithms were applied to simulations of both operations of the blind and of the switchable glazing. The configurations compared were an electrochromic glazing and a roller blind, the controllers used were rule-based, proportional-integral-derivative (PID), anti-windup PID (aPID) and a model predictive controller (MPC). Particular case studies were examined in the weather conditions of Dublin, Ireland to make comparisons of simulated energy savings and occupancy daylight comfort from the use of electrochromic glazing or a roller blind with those for a double-glazed window. The results suggest that previous studies that simulated electrochromic window as an integrated roller blind in a heating-dominated climate would have overestimated building energy loads, and depending on the controller used, overestimated occupancy daylight comfort.

1. Introduction

Windows provide the benefits of thermal insulation, solar heat gains, daylight, exterior viewing and reduce external noise transmission; they can also be a source of uncontrolled heat loss, glare and uncomfortable thermal asymmetries [1–3]. To reduce cooling loads in sunny/hot climates, excessive solar gain is rejected by fixed window glass coatings. In cloudy/cold climates, highly-insulated windows are used to retain solar heat gain. In temperate/seasonally-varying climates with cold winters and hot summers, less energy-use ensues when solar heat gains and heat losses are modulated by weather-adaptive features such as movable shading, shutters and openable windows [4,5].

For dwellings and offices where facades are adaptive to permuting conditions and requirements, they can help optimize indoor conditions to safety occupant comfort while minimizing building energy use. Adaptive building façades combine features, materials and technologies that can change their properties to modulate, convert, and store energy and mass flows according to changing weather conditions and internal comfort requirements [6]. Switchable-transmittance windows can minimize combined annual heating, cooling and lighting energy loads in highly thermally-insulated and airtight buildings, by controlling solar heat gain [7,8].

Electrochromic windows (i) require power only during switching, (ii) retain their optical transparency without a voltage being applied for 12h–48h, (iii) require a low voltage to switch, (iv) have long life switching cycling ability (typically 10^5 cycles), (v) can provide both visible and solar control and (vi) can vary in colour (typically blue or colour neutral). Their switching speed, in the order of minutes for standard sized windows, depends on the window size and temperature [9–12].

For the simulation of switchable windows, various simulation tools and software have been used, each using a different technique(s) to represent a switchable window. Electrochromic windows have been simulated as (i) a switchable window (SW) simulated with all glazing layers present. (ii) a blind: where the electrochromic glazing is simulated as if it were an integrated internal roller blind, and (iii) a combination of both previous techniques. There to-date has been no rigorous comparison of the outcomes of (i) different ways of simulating a switchable window and (ii) each of these ways of simulating a switchable window combined with different control algorithms. There is thus no general agreement on the most effective controller type to be used

* Corresponding author. School of Electrical and Electronic Engineering, Technological University Dublin, Ireland.
E-mail address: d19126291@mytudublin.ie (H. Alkhatib).

https://doi.org/10.1016/j.rineng.2023.101467
Received 13 August 2023; Received in revised form 19 September 2023; Accepted 27 September 2023
Available online 28 September 2023

Nomenclature

Symbol	*Definition*
K_p	Proportional component
K_i	Integral component
K_d	Derivative component
T_i	Derivative time
T_d	Integration time

with switchable windows. This chapter examines the accuracy of simulating a switchable window as a blind and explores the wide range of controller types used with switchable windows, utilizing data from the solar test cell located in Dublin, Ireland. The energy consumption of the test cell and the daylight comfort of occupants were examined using IDA ICE dynamic building simulation software [13]. The study will be done using electrochromic windows simulated either as such or as a blind. The glazing will be controlled by seven different controllers.

This paper is organized as follows.

(i) Section two provides the background and contexts.
(ii) Section three presents the methodology used.
(iii) Section four shows the main findings.
(iv) Section five draws conclusion from this study.

2. Background

Most studies have investigated the performance of electrochromic windows using dynamic building simulations. Particular simulation tools use different techniques to simulate an electrochromic glazing. These techniques can be summarized into three categories (i) blind, (ii) electrochromic (EC) or (iii) a surrogate. The types of simulation used previously to investigate the performance of electrochromic windows are summarized in Table 1 [14–19].

A specific set of control parameters is used in a control algorithm to modulate outputs to achieve desired conditions in an electrochromic window. control parameter data is provided by sensors that measure the required parameter(s) at an appropriate sampling interval. Control parameters used include: (i) solar radiations [20], (ii) outdoor temperature [21], (iii) indoor temperature [22,23], (iv) indoor luminous intensity [24] and (v) heating and cooling loads [16].

2.1. Controller types

As shown in Tables 1 and in previous studies different controllers have been used to control switchable windows. There has been no agreement on the most effective controller type. This study used seven controller types out of these. The selection of controllers for building energy simulations was driven by the need to accurately represent real-world scenarios while considering the specific characteristics of the simulated environment. Each controller was chosen for its unique attributes and relevance. Rule-based controllers were selected due to their simplicity and interpretability. These controllers rely on a set of predefined rules, making them suitable for scenarios where intuitive decision-making is essential. In building energy simulations, rule-based controllers can mimic human-like responses to environmental changes, providing valuable insights into practical control strategies. Proportional-Integral-Derivative (PID) controllers are widely used in various industries, including building automation. Their selection was motivated by their ability to strike a balance between responsiveness and stability. PID controllers can effectively regulate environmental conditions by adjusting control inputs based on error, integral of error, and derivative of error. Their versatility and well-established performance make them a suitable choice for building energy simulations. The inclusion of an Anti-Windup PID (aPID) controllers was driven by the need to address practical issues such as control saturation. In real building systems, actuators may have limitations, and controllers must handle such constraints. The aPID controller, equipped with anti-windup mechanisms, prevents integrator windup during control saturation, ensuring more realistic and robust simulations. Model Predictive Controller (MPC) was chosen for its advanced predictive capabilities. This controller utilizes a dynamic model of the building and considers future predictions when making control decisions. MPC is particularly relevant in scenarios where optimal control strategies need to be determined in real time while considering the system's dynamics and constraints. Its ability to adapt to changing conditions and optimize energy usage aligns with the goals of building energy simulations. Table 2 summarizes the advantages, disadvantages and main features of seven controllers that were investigated in this study.

In the simulation, each of the seven controller types was applied to control the EC glazing and to control the blind. The EC was controlled by the sensed luminous intensity in the zone as shown in Fig. 1. Three thresholds selected by optimization were used. When the sensed luminous intensity crosses the first threshold, a signal was sent from the controller to activate (i) intermediate state I for EC or (ii) a specific blind position and the process was repeated for all EC states and blind positions.

2.1.1. Rule-based

A Rule-Based-Control or On/off controller is the most used strategy for controlling active glazing systems [26–29], Rule-based controller requires source(s) of data and "if statement" rules to manipulate that data. On/Off controllers have only two states: fully on and fully off. In this study, the on/off controller works by sending either 0 or 1 as a signal for electrochromic each state or blind position.

2.1.2. P, PI and PID

A PID controller, widely used residential buildings, is a feedback controller, consisting of three terms (i) proportional (P), (ii) integral (I) and (iii) derivative (D). Each dependent on the error value between the input and the output values. K_p, K_i and K_d are P, I and D parameters respectively. As shown in Equation (7), a change in these parameters will result in a change in the system response [30,31].

$$\text{Output} = K_p \times e(t) + K_i \times \int_0^t e(t)dt + K_d \times \frac{d_e}{dt} \tag{7}$$

where e is the error value. K_p and K_d can also be written as shown in Equation (8) and Equation (9).

$$K_i = K_p \times T_i \tag{8}$$

$$K_d = K_p \times \frac{1}{T_d} \tag{9}$$

where T_d and T_i are, respectively, the derivative time and integration time. Tuning these PID terms to their optimal values is crucial. Tuning techniques used for a PID controller are either; Classical techniques, where an assumption is made about controller parameters and then the PID parameters are manually tuned to achieve the desired output, or computational optimization techniques, where data modelling and a function is used. These optimization techniques need to minimize a function, the function can be energy needs, cost or emissions [32].

In this study, P, PI and PID controllers were examined separately, only PI and PID were tuned using GenOpt software. GenOpt was used to optimize K_p, K_i, K_d parameters, the integration time and derivative time. The optimization was set to the heating, cooling and lighting energy consumption. In this study, for the PI controller, the T_i and the K_i were tuned. and for the PID controller, K_i, K_d, T_i and T_d were tuned.

Table 1
Previous studies on controlling EC windows considering their visual transmission (VT) and solar heat gain coefficient (SHGC).

Case Study	Location	Climate	EC window properties	Simulation type (Blind, EC or a surrogate)	Controller Type	Comfort Conditions	Energy benefit	Software used	Ref
Two zones in PASSYS test cell. Compare the energy performance of an electrochromic window under various control strategies.	Vaulx-en-Velin, France	Oceanic	No. of glass panes: 2 U-value: 1.4 VT: [0.32–0.50] SHGC: [0.22–0.36]	A surrogate: combination of different simulation tools	On/Off PID	Indoor temperature: 21–26 °C. Inside daylight: depends on the strategy used.	Fuzzy controllers reduce heating/ cooling and lighting energy consumption by 4% compared to the ON/OFF controller.	SIBIL building toolbox environment	[14]
Office zone. Evaluate energy consumption using quasi-optimal, predictive and rule-based control strategies.	Montreal, CA	warm-summer humid continental	No. of glass panes: 2 U-value: 1.63 VT: [0.015–0.621] SHGC: [0.09–0.47]	A surrogate: combination of different simulation tools	On/Off Generic algorithm MPC	Indoor temperature: 21–25 (±3) °C. Inside daylight: schedule to keep it on 500 lux	Total building energy consumption reduced by 4%–10% depending on the control strategy.	TRNSYS, EnergyPlus MATLAB	[15]
One zone of 34.8m^2. Development of a comparison-based control strategy.	Anderson, USA	Humid subtropical	No. of glass panes: 2 U-value: Not given VT: [0.10–0.58] SHGC: [0.13–0.40]	A surrogate: combination of different simulation tools	On/Off	Indoor temperature: 22.2–24.4 °C. Indoor daylight: 300–500 lux.	Basic scenarios strategy which uses CP 1 was slightly better than with CP 2.	DIVA-for-Rhino, EnergyPlus MATLAB	[17]
Office building. Evaluate control strategies for different smart window and coating combinations.	Stockholm, Denver and Miami	Oceanic, humid continental, tropical monsoon	No. of glass panes: 2 U-value: 2.8 VT: [0.12–0.74] SHGC: Not given.	Blind	On/Off	Balance temperature: 8–14 °C. Inside daylight: depends on the strategy used.	Occupancy based control is beneficial. The best coating combination differs depending on the balance temperature of the building.	Winsel	[16]
One zone of 48m^2. Compare the energy saving potential of adaptive and controllable smart windows.	Trondheim, Madrid, and Nairobi	Oceanic climate, Mediterranean climate, subtropical climate	No. of glass panes: 2 U-value: [1.1–1.6] VT: [0.30–0.90] SHGC: [0.10–0.45]	Blind	On/Off PI	Indoor temperature: 21–25 °C. Indoor lighting: schedule with range of 100–500 lux.	Lowest building energy consumption using electrochromic windows controlled by the operative temperature.	IDA ICE	[19]
Office building (mid-size) Compare four individual control parameters.	Six locations in USA	Climates are split between Marine, Dry and Moist	No. of glass panes: 2 U-value: [3.2–6.3]. VT: [0.10–0.72] SHGC: [0.10–0.50]	EC	On/Off	Indoor temperature: 20–24 °C. Indoor daylight: schedule.	Energy consumption was 17.4% lower using outdoor temperature compared to the other three CP.	EnergyPlus	[18]
One room of 25m^2 Integration of smart windows into building design	Quebec City, Canada	Continental Climate	No. of glass panes: 2 U-value: [1.36–2.5] VT: [0.58–0.78] SHGC: [0.36–0.73]	EC	MPC	Indoor Temperature: 20 °C. Indoor lighting: schedule to keep it on 400lux.	Energy consumption was reduced between 8% and 53% depending on the orientation.	eQUEST MATLAB	[8]
High rise building Energy consumption of high rise using smart windows and other tools.	Four locations in Iran.	Hot-summer mediterranean, cold semi-arid steppe, hot desert and hot semi-arid climates[b]	No. of glass panes: 2 U-value: [1.32–2.5] VT: [0.099–0.78] SHGC: [0.11–0.7]	EC	On/Off	Indoor Temperature: 20 °C. Indoor lighting: Maximum allowable glare index of 22	Energy consumption was reduced by 35.5% using EC and other tools.	EnergyPlus DesignBuilder	[25]

Table 2
advantages and disadvantages of the controller types examined [4].

Controller type	Advantages	Disadvantages	Accuracy	Complexity	Computational requirements
Rule-Based	Simple, no tuning required.	Overshoots the desired condition	Lack precision in situations where complex decision-making is required	Relatively simple	Computationally lightweight and require minimal resources.
Proportional (P)	Reduced rise time is required to achieve the desired tinting level; no tuning is required in most cases.	Has a significant overshoot. Takes a long time to stabilize.	Can achieve good accuracy for a wide range of systems but may struggle with highly nonlinear systems or systems with significant time delays	Moderately complex due to the need for tuning coefficients, and tuning can be challenging for complex systems.	Low to moderate computational requirements and can be implemented efficiently.
Proportional-Integral (PI)	Less rise time with controlled overshooting.	Causes minor overshoot and instability. Tuning required.			
Proportional-Integral-Derivative (PID)	No overshooting, very stable.	Slow response, tuning required.			
Anti-Windup Proportional-Integral (aPI)	Eliminates the delay that can be caused in the PI controller.	Can be unstable, can overshoot, more tuning compared to normal PI.	Addresses integrator windup but may still struggle with systems that have extreme saturation conditions or nonlinearity.	Slightly more complex than standard PID controllers due to the anti-windup mechanisms.	Have similar computational requirements to PID controllers.
Anti-Windup Proportional-Integral-Derivative (aPID)	Eliminates the delay that can be caused in the PID controller.	Significant tuning is required.			
Model Predictive Controller (MPC)	Predicts future changes and accommodates disturbances.	Requires (i) system modelling (ii) training and (iii) validation.	Can provide high accuracy as it considers system dynamics and future predictions. However, it relies heavily on accurate system models.	The most complex among the controllers, as it involves solving optimization problems at each time step.	Demands significantly higher computational resources than the other controllers due to its optimization-based approach.

2.1.3. *Anti-windup PI and PID*

A PI/PID windup problem causes saturation to the actuator which causes instability. It ensues when the error (i.e., the difference between input and output) is either large or remains nonzero for a long time. A PI/PID controller under saturation usually gives a delayed response to the input change, the deeper the saturation level the more delay is added to the response [33].

Anti-windup controllers have been used in different applications, in this study, the tracking anti-windup scheme shown in Fig. 2 was used. This type of anti-windup controller prevents the integral term from accumulating a large value by using an extra component (represented by the green line in Fig. 2) which sense the difference between the output and input multiplied by tracking gain to the integral gain.

The model, an extension of "Modelica.Blocks.Continuous.LimPID", offers P, PI, PD, and full PID control modes with adaptable "reverseAction" for heating or cooling. It includes features like output limiting, anti-windup, and setpoint weighting for versatile control system modelling. For the anti-windup PI controller, the derivative gain was set to zero and T_i, K_i, tracking-gain and limiter were tuned. For the anti-windup PID controller, T_i, K_i, K_d, both tracking-gain and limiter were tuned.

2.1.4. *Model predictive control*

Model Predictive Control (MPC) calculates the ideal inputs for the controller in order to minimize the overall objective over a finite prediction horizon. Previous studies have shown that MPC can significantly reduce energy consumption by 15%–50% [35–37].

Building an accurate underlying building simulation model is crucial

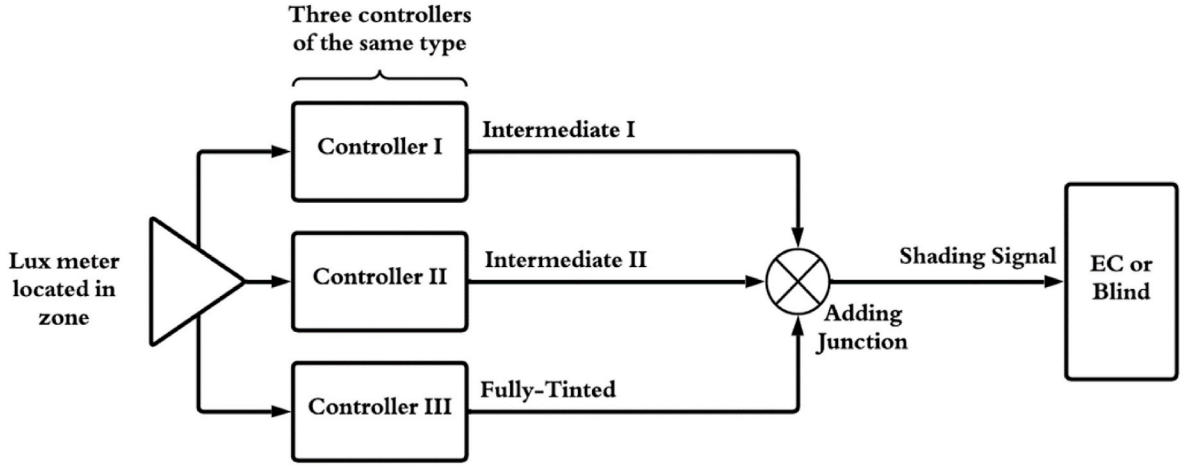

Fig. 1. Control model for EC glazing and blind.

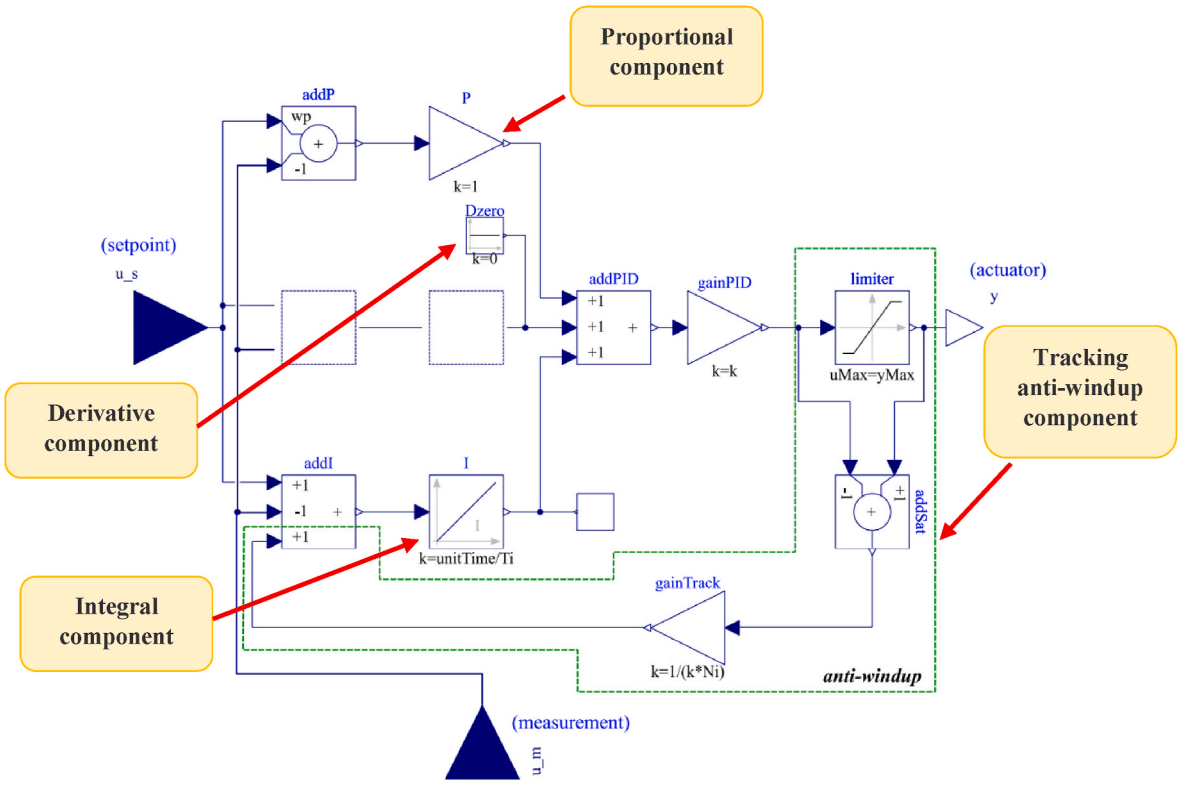

Fig. 2. The anti-windup PI/PID Controller modelled in this study (adapted from Ref. [34]).

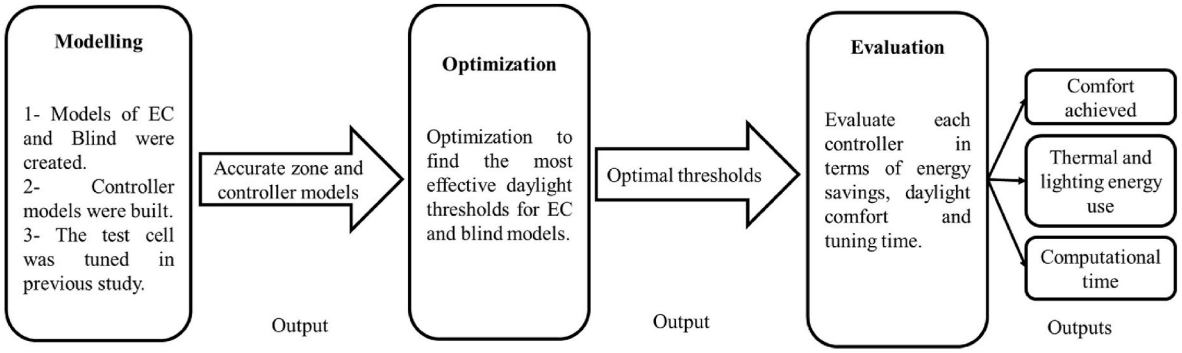

Fig. 3. Methodology.

for the performance of the MPC strategy. While a detailed physical model can accurately represent nonlinear and discontinuous processes in a building, using complex models (i) increases the computational demand and (ii) is not suitable for use in the multiple simulations associated with optimization algorithms. A trade-off between simplicity and accuracy is, therefore, necessary [38,39]. There are three types of building simulation model paradigms used with MPC.

(i) "White-box" models of dynamic building behaviour calculated from physical principles of heat transfer and conservation of energy and mass [38],
(ii) "Black-box" models that learn dynamic building behaviour from measured data without underlying physical relationships [39].
(iii) "Grey-box" models which are physical models simplified using a space state model, performing parameter estimation from measured data. The typical concept in a Grey-box model involves the use of resistor and capacitor (RC) analogies, which simplifies the building envelope into first-order ordinary differential equations [40].

Which of these three is appropriate depends on the outcomes sought and available data [41].

3. Methodology

Fig. 3 summarizes the methodology used in this study. The methodology comprises of three stages: (i) modelling the zone and the control strategies, (ii) optimizing for the optimal threshold and (iii) Evaluation using annual simulations.

An experimental solar test cell located in Dublin (53.3° N, 6.26° W) was used in this study. Fig. 4 shows the south facing façade of the solar test cell. The cell designed to evaluate the performance of adaptive façade technologies, consists of three rooms; room number one (highlighted in red lines) was used in this study. Overall heat loss coefficients of the fabric were measured and used as an input to the simulation. The IDA Indoor Climate and Energy (IDA ICE) software or simulating building indoor climate and energy characteristics [19,42] was used in this study based on its capability (i) to log the output values of variables, (ii) to perform various pre-defined control strategies and (iii) to develop

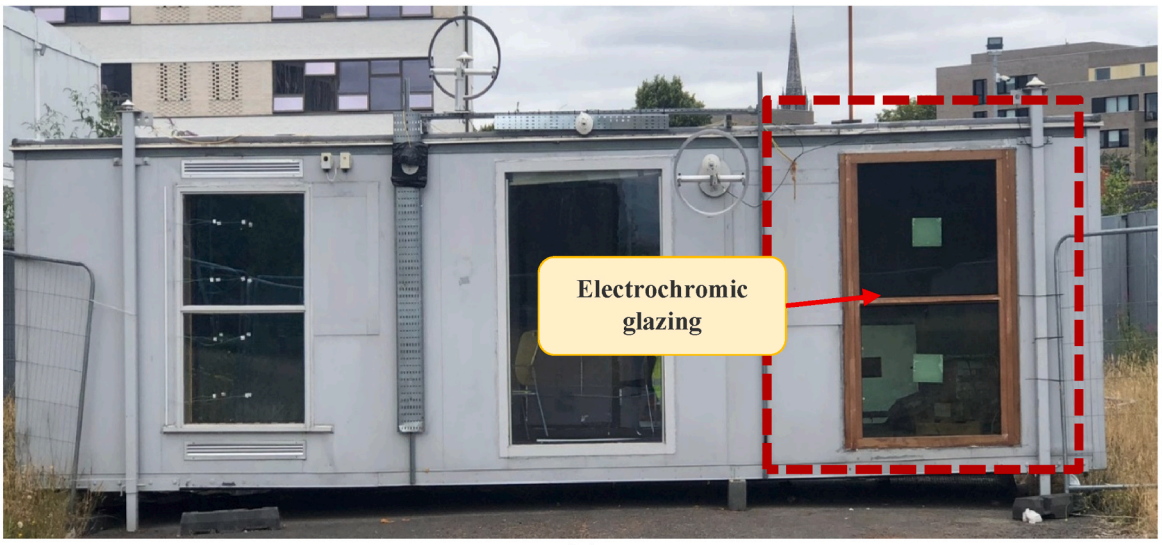

(a)

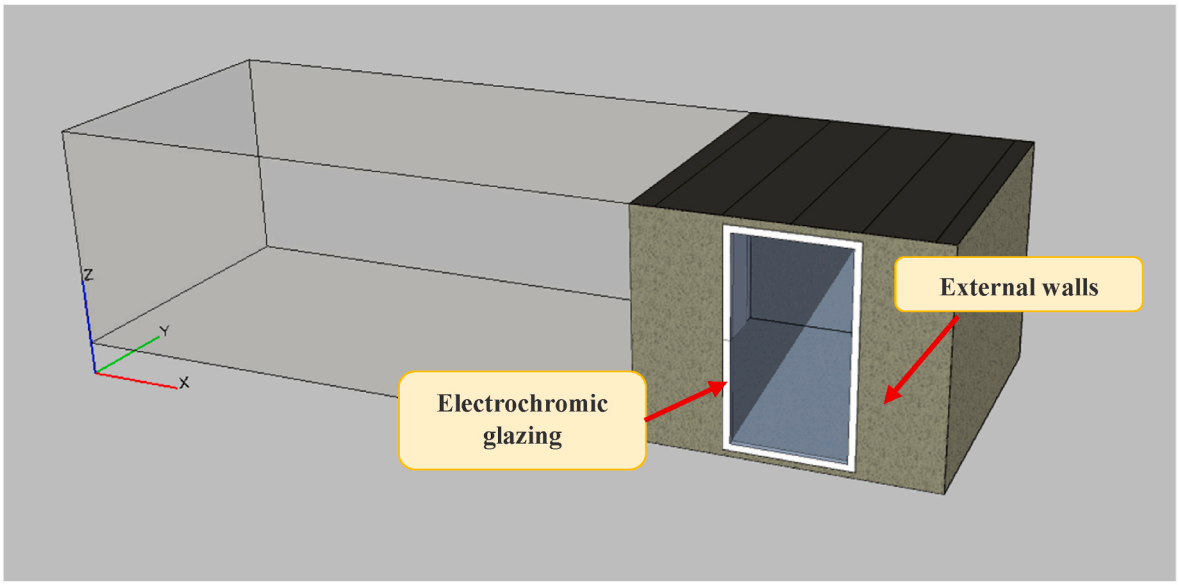

(b)

Fig. 4. (i) Solar test cell in Dublin, (b) Solar test cell model in IDA ICE.

Table 3
Electrochromic window properties in different tinting states.

Electrochromic				Blind
Solar Factor g	Light Transmission τ_{vis}	U-value (W/m^2.K)	Level of Tint for EC and Blind	Corresponding Blind Position
0.41	0.62	1.1	Clear	Fully Open
0.12	0.17		Intermediate I	1/3 of the way down
0.06	0.05		Intermediate II	2/3 of the way down
0.05	0.01		Fully Tinted	Fully closed

custom control algorithms (including Modelica models) that will be exploited in Section 4. The IDA ICE model was calibrated and validated against experimental data in previous study on adaptive building façade [29]. This was done by running the experimental data for a week. External weather conditions were imported into the simulation model. the model were then tuned by comparing measured indoor temperatures to predicted indoor temperatures from the simulations model during the first three days. The next four days of the week were then used for validation.

A SageGlass Electrochromic (EC) window in two parts separated by a transom was installed in the south façade as shown in Fig. 4. The EC glazing has four different switching states with corresponding blind positions shown in Table 3. The window with a blind structure is shown in Fig. 5. The windows' properties were taken from SageGlass manual.

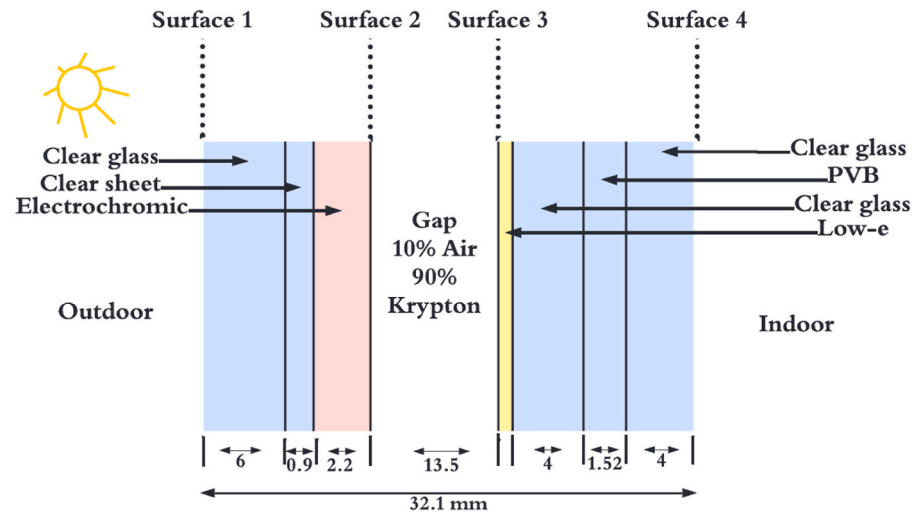

(a)

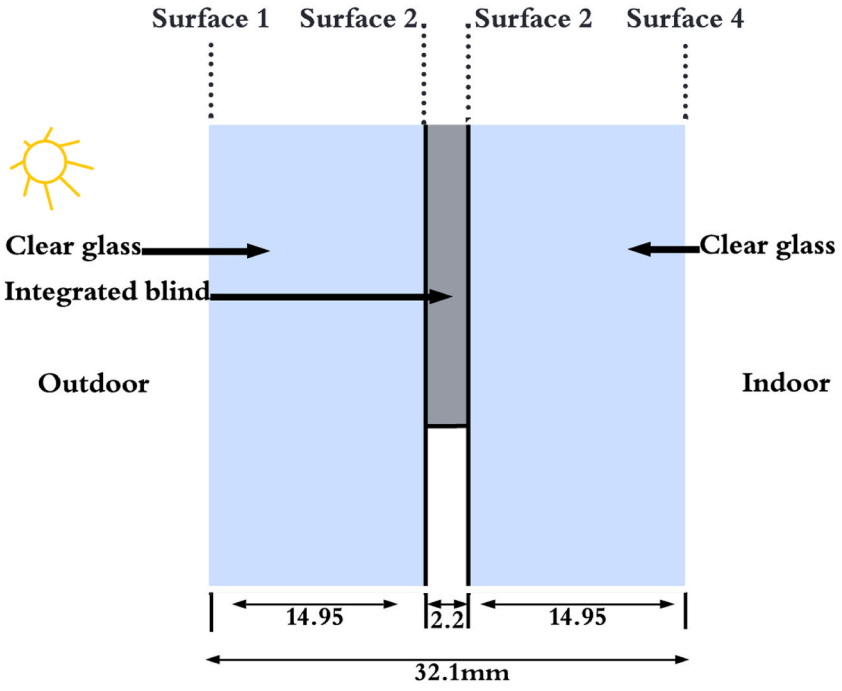

(b)

Fig. 5. (a) Electrochromic window, (b) Window with blind structure.

To enable comparison the electrochromic and blind models were given the same properties. Fig. 6 shows an example of switchable window being at the intermediate I state and the corresponding blind position. Fig. 7 shows how incident solar irradiance is reflected, absorbed and transmitted in Electrochromic glazing simulation and in blind integrated simulations. The main difference in both simulations is that different blind positions are typically used to simulate different electrochromic states, this means that partial reduction of transmission across the window by an electrochromic is assumed to be the same as full shading of a part.

Ideal heater and cooler were selected in IDA ICE. They have no physical representation inside the zone. Meaning that energy produced by the systems was generated in the middle of the zone and spread equally throughout. Since the heating/cooling optimum start/stop is out of the scope of this article, a 10 kW heating/cooling capacity to always be able to achieve the required temperature set points and to avoid any thermal discomfort at the beginning of the working hours. The efficiencies of both the heater and the cooler were assumed to be 100%. Losses due to the thermal bridges were accounted for in the simulation. Three internal gains are defined as follows.

(i) Two lighting units of 350 W with an efficacy of 20 lm/W are positioned at the centre of the building model.
(ii) Indoor equipment producing 200 W of heat.
(iii) Two occupants with a metabolic rate for each person are set to 1 metabolic equivalent task (met) [19,43].

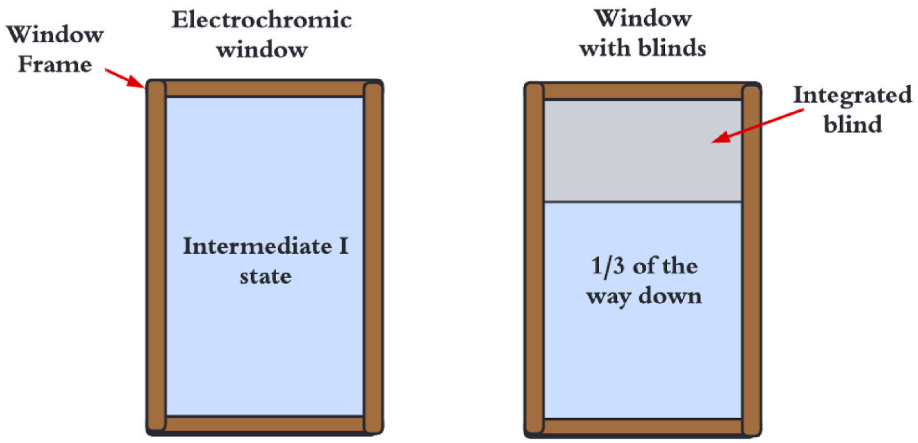

Fig. 6. Intermediate I state with the corresponding blind position.

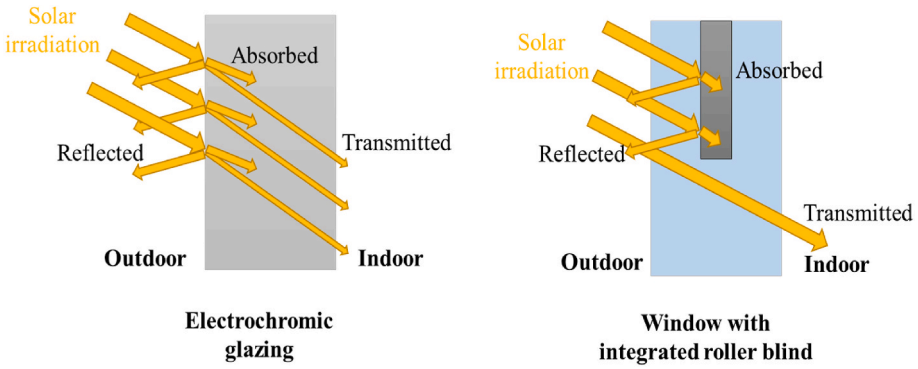

Fig. 7. Incident solar irradiance on electrochromic glazing and integrated roller blind.

Table 4
Luminous intensity threshold with corresponding tinting level and blind position.

Electrochromic		Blind	
Luminous intensity (lux)	Corresponding EC tinting level	Luminous intensity (lux)	Corresponding blind position
787>	Clear	853>	Fully Open
787	Intermediate I	853	1/3 down
933	Intermediate II	985	2/3 down
1201	Fully Tinted	1354	Fully closed

The heating and cooling units inside the zone will be set to keep the temperature inside the comfort range 18 °C–21 °C based on ANSI/ASHRAE Standard 62.1 and ANSI/ASHRAE Standard 55 [44,45]. The heating and cooling loads was calculated depending on the energy consumption.

Following the British Standards Institution (BSI) standards [46,47], to maintain daylight discomfort and avoid glare the average illuminance in the zone should be between 200 and 500 lx at a height of 1.2 m above the floor level [48,49]. The range identified in BSI standard is a conservative limit so does not mean that illuminance levels above the limit will eventually result in glare [47]. The number of hours for which the average illuminance is not between 200 and 500 lx during the work hours was calculated. Outside the scheduled occupancy time (06h–18h) and on weekends, there is no constraint on the targeted indoor lighting and thermal comfort meaning that no lighting, heating and cooling energy consumption occur.

4. Results

4.1. Threshold optimization

Four different indoor daylight luminous intensities that activate a specific window tint or blind position were examined. For each tinting state and blind position, an optimization process was done using GenOpt sought to find the most effective control strategy that resulted in the least heating cooling and lighting energy consumption. GenOpt is a generic optimization program, written in Java, typically used for minimizing a specific value by coupling it with an external simulation software such as IDA ICE [13]. GenOpt has multiple optimization algorithms that can deal with discrete and continuous variables to probabilistically identify simulation objectives optima. For the optimization, a range from 0 lx to 3000 lx and an initial point of 500 lx were set. Table 4 shows the EC tinting level and blind states with the corresponding luminous intensity threshold.

4.2. Model predictive control training

A grey-box model was used in this study with the RC model shown in Fig. 8. The RC model consists of (i) external walls, roof, ground, window and other components which separate the indoor from the outdoor environment. Building envelope model includes heat transfer through (i) conduction from walls and windows, (ii) convection from walls and infiltration and (iii) radiation (solar gains), (iv) HVAC system and internal gains and (v) Weather and occupancy [8,50,51]. The following assumptions were made.

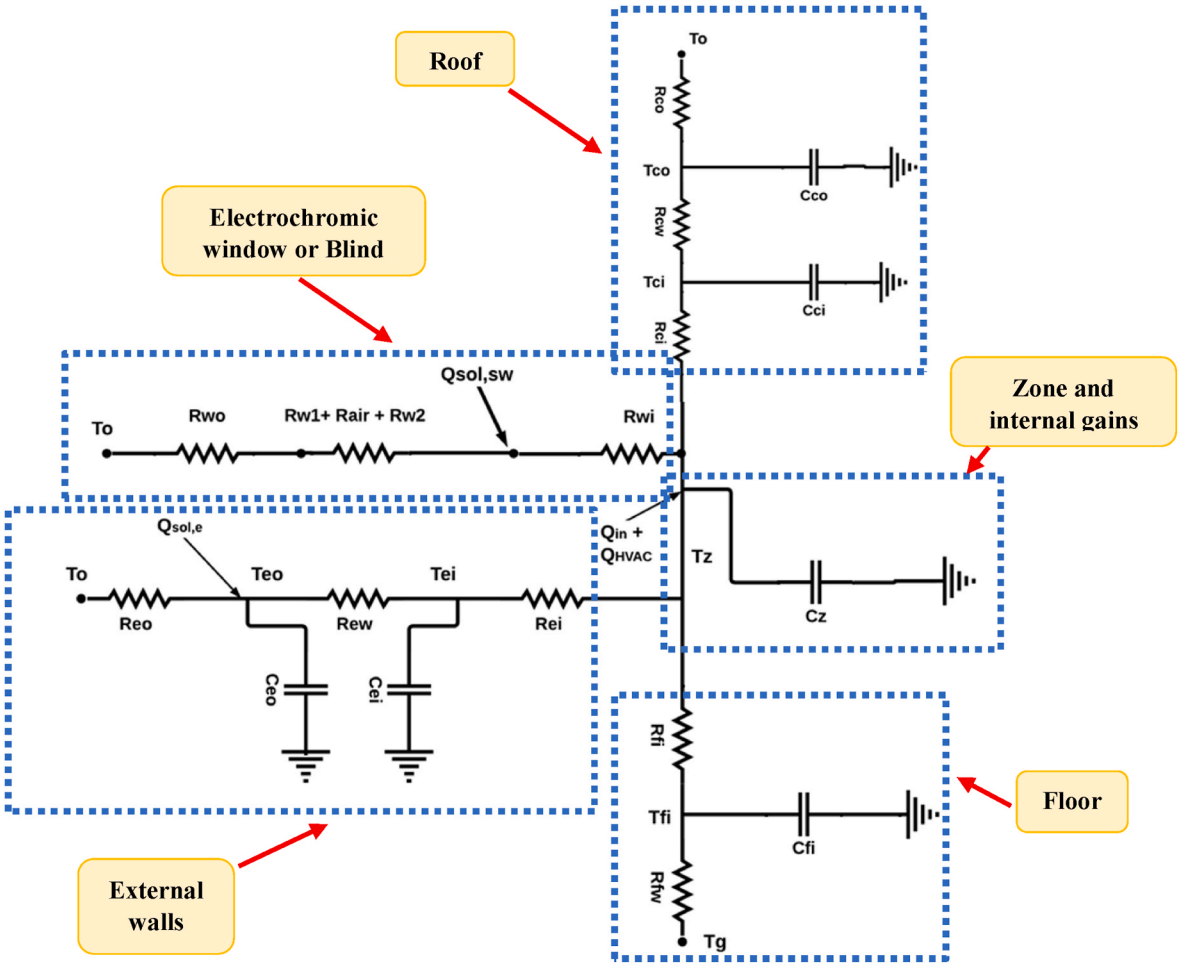

Fig. 8. Overall RC model for the building model.

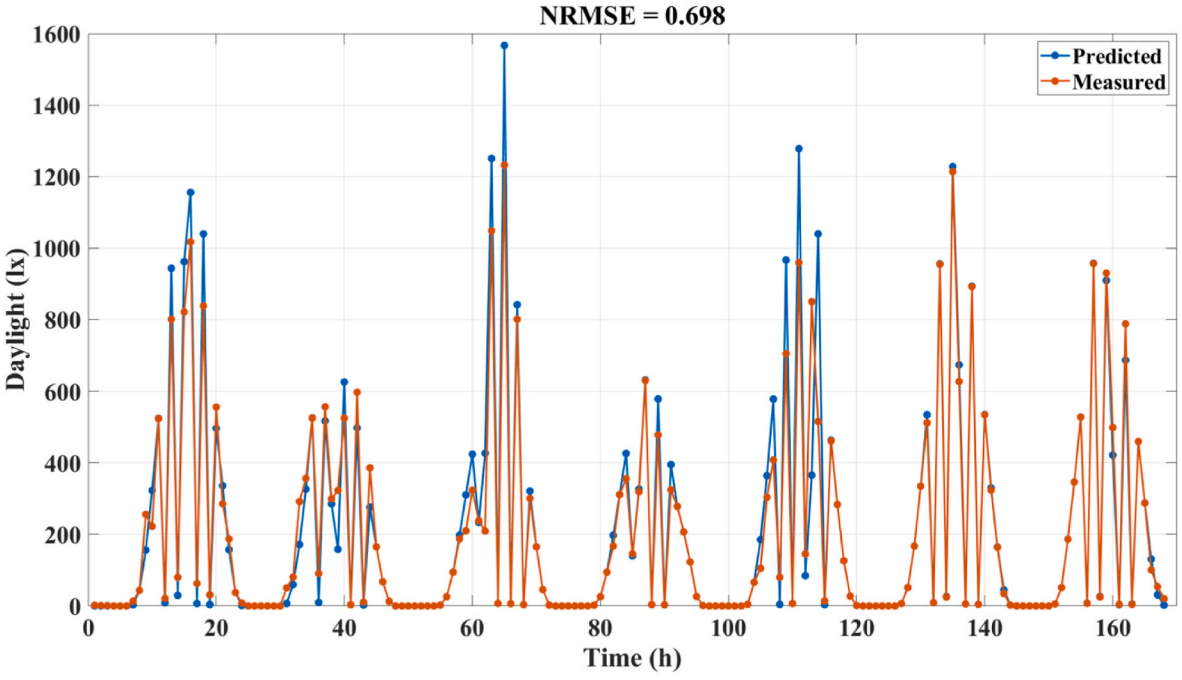

Fig. 9. Predicted and measured luminous intensity.

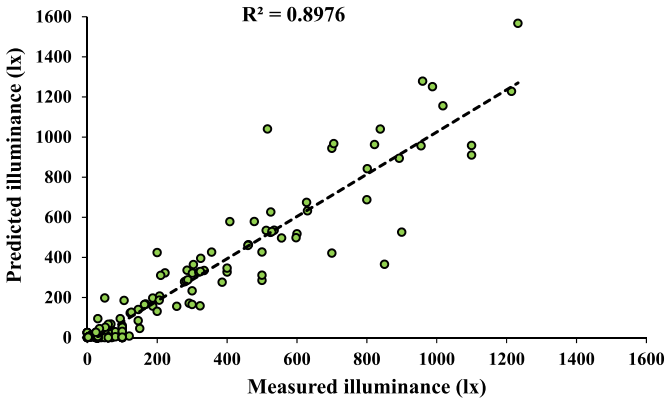

Fig. 10. Relationship between predicted and measured indoor illuminance.

- Air inside the simulated room is well mixed, so the interior air temperature is uniform across the zone.
- One dimensional heat transfer is assumed for the walls and surfaces, with no lateral temperature differences, allowing walls to be denoted by one temperature.
- External wall does not reflect radiation diffusely.
- Internal wall surface temperatures are the same as the inside air temperature.

RC model equations were converted to matrixes used for training process.

Building air and wall temperatures, solar radiation and heat input data that captures building dynamics is necessary for the model. In this study, this data was obtained from outputs from building simulation model in IDA ICE. Three weeks of data hour-by-hour were used to train the controller model, simulation data for one week was used to validate the training process. Fig. 9 shows predicted and simulated luminous intensities during the latter validation week for an EC glazing. The Normalized Root Mean Squared Error (NRMSE) was used to difference between the simulated and predicted luminous intensity. The selection of the Normalized Root Mean Square Error (NRMSE) as the evaluation metric in this study is driven by its suitability for addressing the specific objectives of the research. NRMSE is a widely used metric in various fields, including building energy simulations. It standardizes the error metric by dividing the root mean square error (RMSE) by the range of the data. This standardization allows for comparisons across different datasets and scenarios, making it a suitable choice for assessing the performance of controllers across various building energy simulation scenarios.

The NRMSE between the simulated or predicted luminous intensity was 69.8% for simulation of the EC glazing and 73.6% for simulation of the blind. The correlation R between the measured and predicted indoor air temperature was 0.89 as shown in Fig. 10. This means that both have a strong uphill (positive) linear relationship. It can be seen that prediction accuracy decreases with higher illuminance levels.

4.3. Controllers' comparison

To give an example of the shading signal, indoor temperature change and the luminous intensity inside the zone, for rule-based and model-predictive controllers, an intermediate day (between a sunny and a cloudy day) was selected to make the comparison. It should be noted that while the intermediate day approach provides valuable insights into typical conditions, it may not fully capture the range of performance scenarios encountered over a year. Fig. 11 shows the outside temperature and solar radiation. Fig. 12 Shows the shading signal, indoor temperature and indoor luminous intensity using a simulation of EC glazing or using a blind to simulate the switchable window. The temperature change was significant using a blind compared to EC glazing, that is because of the blind capability to completely block daylight coming into the zone. The inside daylight changed notably between using a blind and an EC in both controller types. The shading signal gradually changed between the window states using MPC compared to a rule-based controller. This has an effect on the window's energy consumption when switching between different states, especially since, in most cases, the window controlled by MPC did not reach Intermediate II and fully-tinted states (see Table 4).

4.4. Tuning time

Computational tuning time is the amount of time it took the computer system to optimize for the optimal controller values. Relative computing time is the computational time relative to MPC tuning time (longest time). Relative computing time does not depend on the computer specifications, this means that relative computing time taken as percentage can be applied to other systems with different specifications. Table 5 shows the computational tuning time and relative computing time of five controllers, the tuning time increased with the greater controller complexity.

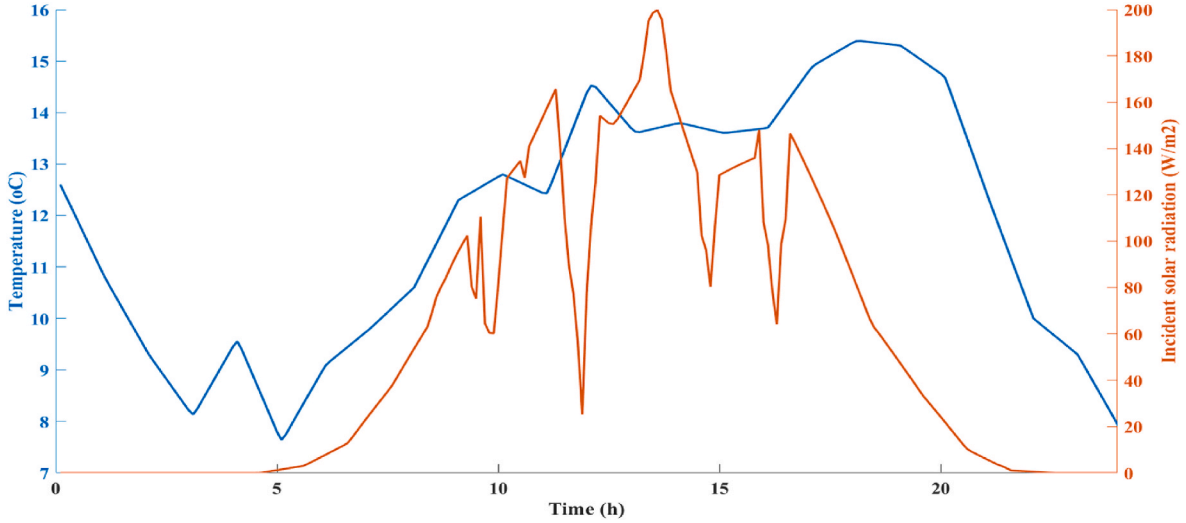

Fig. 11. Total solar radiation on the facade and outside Temperature.

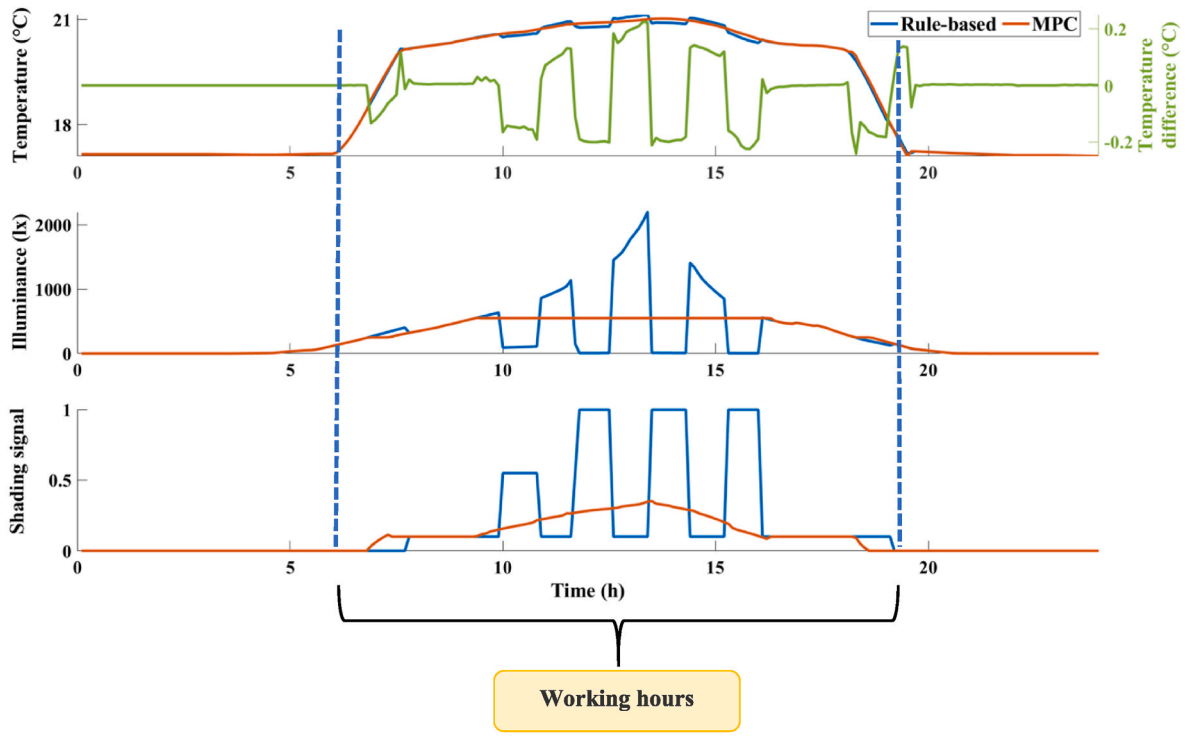

(a)

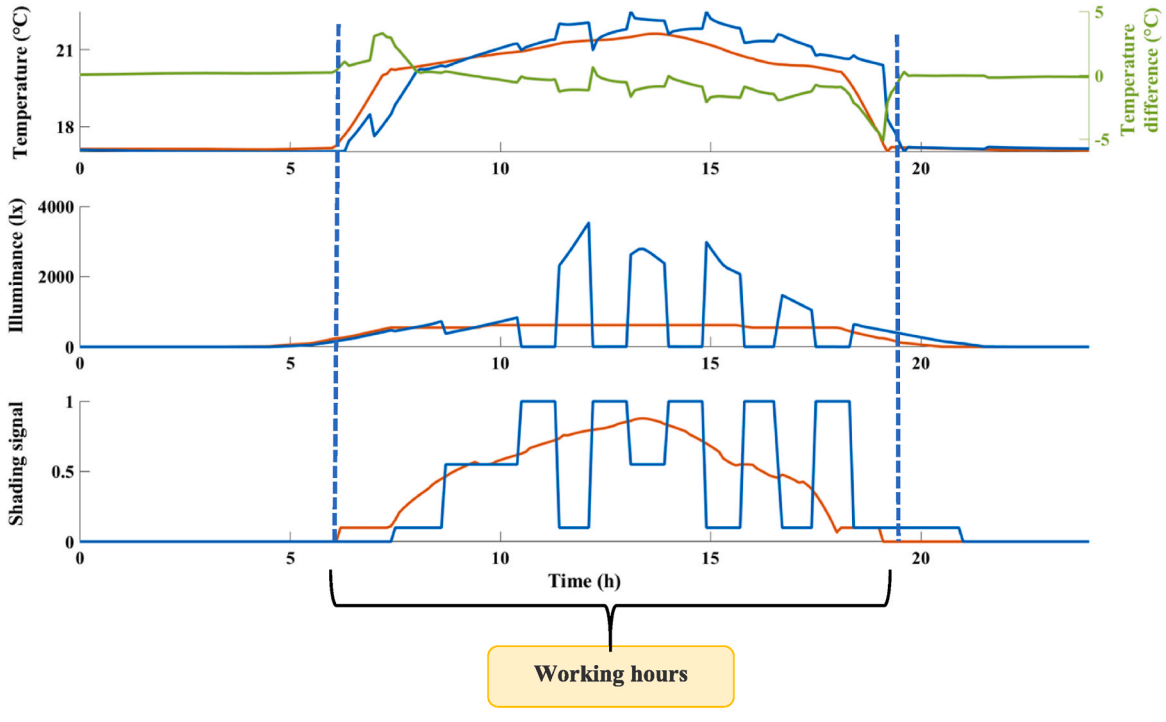

(b)

Fig. 12. Shading signal, daylight and indoor temperature using model predictive control and rule-based controller in (a) EC and (b) blind.

Table 5
Tuning time using different controllers.

Controller type	Electrochromic		Blind	
	Computational tuning time	Relative computing time	Computational tuning time	Relative computing time
PI	1h 02 m	0.18	0h 52 m	0.21
PID	2h 24 m	0.41	1h 42 m	0.41
Anti-windup PI	3h 35 m	0.61	2h 38 m	0.64
Anti-windup PID	4h 05 m	0.69	3h 21 m	0.81
MPC	5h 53 m	1	4h 08 m	1

4.5. Annual simulations

In this study, seven controllers were examined. For separate simulations each controller was used to manipulate electrochromic glazing transparency and blind position depending on interior illuminance level. Annual heating, cooling, lighting energy consumption and tuning time were calculated for each controller when used separately with an electrochromic window and with a roller blind.

Fig. 13 shows the annual energy consumption of the zone using the seven controllers, for the simulations which were done in the climate of Dublin, Ireland. In this climate annual heating energy consumption is generally higher than lighting and cooling energy consumptions. A switchable window simulated as electrochromic glazing gave lower energy consumption for all seven controllers compared with simulation using an integrated blind. However, as shown in Fig. 13, the controllers rank order in terms of energy needs was the same in both cases, with the Rule-based controller resulting in the higher energy needs and MPC with the least energy needs.

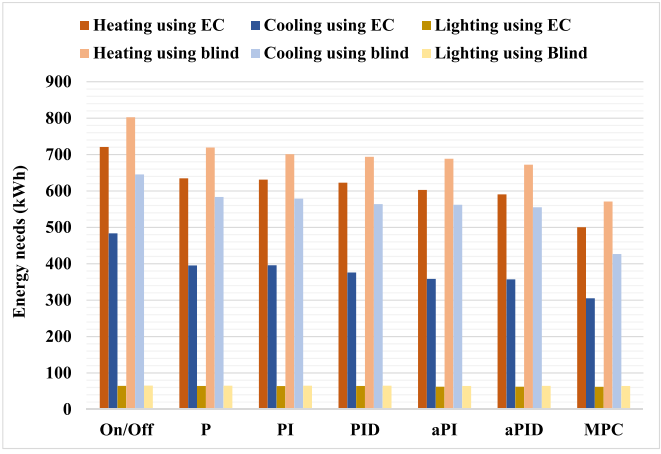

Fig. 13. Annual total heating and cooling energy consumptions for each of seven controllers using an Electrochromic window and a Blind.

Fig. 14 shows the annual daylight comfort and discomfort periods from simulation of a blind and an EC glazing. The comfort period is the amount of time the average indoor illuminance was maintained (Within range) in the comfort range (200–500 lx), and the discomfort periods are the amount of time the average indoor illuminance was below (Under range) or higher (Over range) the recommended range. MPC achieved the most comfort period with an average of 72% daylight comfort achieved during working hours, because MPC predicted the daylight level every hour, so reacted ahead of changes. On the other hand, Rule-based controller caused more daylight discomfort compared to other controller types 58%. The difference between the seven controllers was insignificant when using a blind to simulate the window. However, the difference between the controllers was significant when simulating an EC. This is because unlike the blind where it fully blocks a portion of the daylight in intermediate position as shown in Fig. 7, an EC moderates the transparency of the entire pane.

To provide a base case to calculate energy savings from displaced heating and lighting, two double-glazed windows with the same properties have been used. The energy consumption using the static double-glazed window was 1623 kWh and the daylight comfort was 43% of annual working hours. Fig. 15 shows EC and blind energy savings and daylight comfort increase compared to a double-glazed window.

5. Conclusions

The performance of a roller blind and an electrochromic glazing have been simulated, the different outcomes in performance have been examined for seven different controllers. For the particular conditions studied, a room simulated with an electrochromic glazing required from 1268 kWh to 868 kWh heating, cooling and lighting energy needs depending on controller algorithm, these were equivalent to 22% and 46% energy savings when compared to a double-glazed window. For the same particular conditions, the simulated room with a roller blind required from 1513 kWh to 1062 kWh heating, cooling and lighting

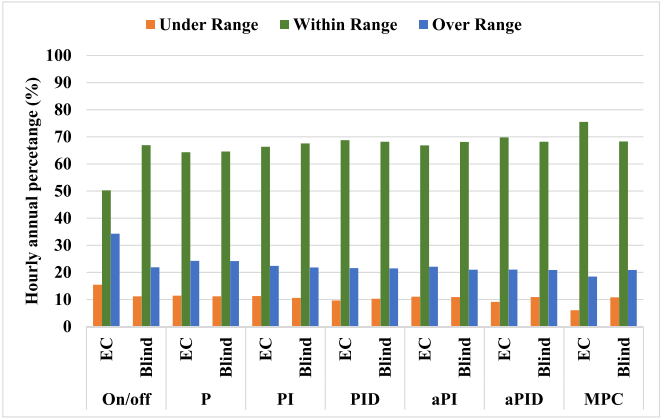

Fig. 14. Annual daylight comfort periods using seven controllers using (a) Electrochromic and (b) Blind.

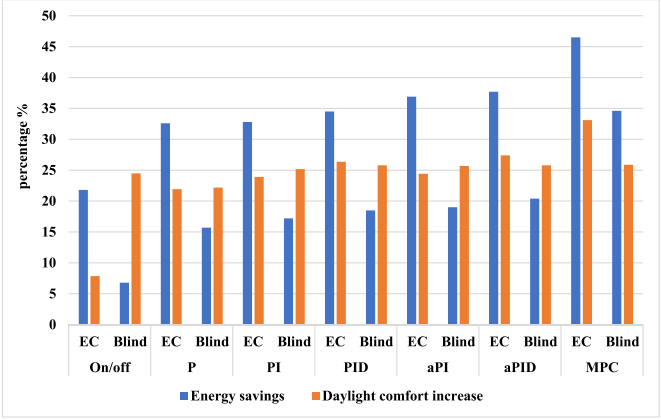

Fig. 15. Energy savings and daylight comfort compared to a double-glazed window.

energy needs depending on the control algorithm, these were equivalent to 7% and 35% energy savings when compared to a double-glazed window. Simulation across seven controllers using blinds resulted in a 27% annual average daylight discomfort compared to a 30% daylight annual average discomfort for the simulation of electrochromic glazing. Moreover, it's essential to highlight the aspect of computational optimization time. The tuning required for EC glazing simulations demanded an average of 3 h and 23 min. In contrast, simulating roller blinds showcased more computational process time, with an average time of 2 h and 32 min. The results of this study suggest that previous studies simulating electrochromic windows as integrated roller blinds in heating-dominated climates may have overestimated building energy loads. Additionally, depending on the controller used, they may have also overestimated occupancy daylight comfort. These findings underscore the importance of simulation method selection and its impact on building performance and occupant well-being.

Declaration of competing interest

The authors declare that they have no known competing financial interests or personal relationships that could have appeared to influence the work reported in this paper.

Data availability

No data was used for the research described in the article.

Acknowledgment

This research was funded by MaREI, the SFI Research Centre for Energy, Climate, and Marine [Grant No: 12/RC/2302_P2]. The author acknowledges the assistance of Max Tillberg of the EQUA Solutions support team in the development of the simulation model used in the study.

References

[1] M. Knoop, O. Stefani, B. Bueno, B. Matusiak, R. Hobday, A. Wirz-Justice, K. Martiny, T. Kantermann, M. Aarts, N. Zemmouri, S. Appelt, B. Norton, Daylight: what makes the difference? Light. Res. Technol. 52 (2020) 423–442, https://doi.org/10.1177/1477153519869758.

[2] C.E. Ochoa, M.B.C. Aries, E.J. van Loenen, J.L.M. Hensen, Considerations on design optimization criteria for windows providing low energy consumption and high visual comfort, Appl. Energy 95 (2012) 238–245, https://doi.org/10.1016/j.apenergy.2012.02.042.

[3] H. Alkhatib, P. Lemarchand, B. Norton, D.T.J. O'Sullivan, Comparison of control parameters for roller blinds, Sol. Energy 256 (2023) 110–126, https://doi.org/10.1016/j.solener.2023.03.042.

[4] H. Alkhatib, P. Lemarchand, B. Norton, D.T.J. O'Sullivan, Deployment and control of adaptive building facades for energy generation, thermal insulation, ventilation and daylighting: a review, Appl. Therm. Eng. (2020), 116331, https://doi.org/10.1016/j.applthermaleng.2020.116331.

[5] United Nations Environment Programme and Global Alliance for Buildings and Construction, 2020 Global Status Report for Buildings and Construction: Towards a Zero-emissions, Efficient and Resilient Buildings and Construction Sector - Executive Summary, Available at:, 2020 https://wedocs.unep.org/20.500.11822/34572. (Accessed 28 September 2023).

[6] G. Capeluto, C.E. Ochoa, Intelligent Envelopes for High-Performance Buildings, Springer International Publishing, Cham, 2017, https://doi.org/10.1007/978-3-319-39255-4.

[7] A. Ghosh, B. Norton, Advances in switchable and highly insulating autonomous (self-powered) glazing systems for adaptive low energy buildings, Renew. Energy 126 (2018) 1003–1031, https://doi.org/10.1016/j.renene.2018.04.038.

[8] J.-M. Dussault, L. Gosselin, T. Galstian, Integration of smart windows into building design for reduction of yearly overall energy consumption and peak loads, Sol. Energy 86 (2012) 3405–3416, https://doi.org/10.1016/j.solener.2012.07.016.

[9] C. Lampert, Smart switchable glazing for solar energy and daylight control, Sol. Energy Mater. Sol. Cell. 52 (1998) 207–221, https://doi.org/10.1016/S0927-0248(97)00279-1.

[10] M. Murphy, A. Gustavsen, B. Jelle, M. Haase, Energy savings potential with electrochromic switchable glazing, in: Conference: Proceedings of the 9th Nordic Symposium on Building Physics (NSB 2011), 2011, pp. 1281–1288. Tampere, Finland, 29 May – 2 June, 2011.At: Tampere, Finland. https://www.researchgate.net/publication/320696693_energy_savings_potential_with_electrochromic_switchable_glazing.

[11] C.G. Granqvist, M.A. Arvizu, İ. Bayrak Pehlivan, H.-Y. Qu, R.-T. Wen, G. A. Niklasson, Electrochromic materials and devices for energy efficiency and human comfort in buildings: a critical review, Electrochim. Acta 259 (2018) 1170–1182, https://doi.org/10.1016/j.electacta.2017.11.169.

[12] H. Alkhatib, P. Lemarchand, B. Norton, D.T.J. O'Sullivan, Optimal temperature-actuated control of a thermally-insulated roller blind, Build. Environ. 244 (2023), 110751, https://doi.org/10.1016/j.buildenv.2023.110751.

[13] M. Wetter, Generic Optimization Program User Manual Version 3.0.0, 2009, https://doi.org/10.2172/962948. Berkeley, California (United States).

[14] M.N. Assimakopoulos, A. Tsangrassoulis, M. Santamouris, G. Guarracino, Comparing the energy performance of an electrochromic window under various control strategies, Build. Environ. 42 (2007) 2829–2834, https://doi.org/10.1016/j.buildenv.2006.04.004.

[15] J.-M. Dussault, M. Sourbron, L. Gosselin, Reduced energy consumption and enhanced comfort with smart windows: comparison between quasi-optimal, predictive and rule-based control strategies, Energy Build. 127 (2016) 680–691, https://doi.org/10.1016/j.enbuild.2016.06.024.

[16] A. Jonsson, A. Roos, Evaluation of control strategies for different smart window combinations using computer simulations, Sol. Energy 84 (2010) 1–9, https://doi.org/10.1016/j.solener.2009.10.021.

[17] M. Hamidpour, V. Blouin, Development of a comparison-based control strategy of electrochromic glazing for the management of indoor lighting and energy efficiency, in: 2018 Building Performance Analysis Conference and SimBuild Co-organized by ASHRAE and IBPSA-USA, 2019. https://www.researchgate.net/publication/330657614_development_of_a_comparison-based_control_strategy_of_electrochromic_glazing_for_the_management_of_indoor_lighting_and_energy_efficiency.

[18] J. Hoon Lee, J. Jeong, Y. Tae Chae, Optimal control parameter for electrochromic glazing operation in commercial buildings under different climatic conditions, Appl. Energy 260 (2020), 114338, https://doi.org/10.1016/j.apenergy.2019.114338.

[19] R. Tällberg, B.P. Jelle, R. Loonen, T. Gao, M. Hamdy, Comparison of the energy saving potential of adaptive and controllable smart windows: a state-of-the-art review and simulation studies of thermochromic, photochromic and electrochromic technologies, Sol. Energy Mater. Sol. Cell. 200 (2019), 109828, https://doi.org/10.1016/j.solmat.2019.02.041.

[20] F. Gugliermetti, F. Bisegna, Visual and energy management of electrochromic windows in Mediterranean climate, Build. Environ. 38 (2003) 479–492, https://doi.org/10.1016/S0360-1323(02)00124-5.

[21] J. González, F. Fiorito, Daylight design of office buildings: optimisation of external solar shadings by using combined simulation methods, Buildings 5 (2015) 560–580, https://doi.org/10.3390/buildings5020560.

[22] M. Scorpio, G. Ciampi, A. Rosato, L. Maffei, M. Masullo, M. Almeida, S. Sibilio, Electric-driven windows for historical buildings retrofit: energy and visual sensitivity analysis for different control logics, J. Build. Eng. 31 (2020), 101398, https://doi.org/10.1016/j.jobe.2020.101398.

[23] V. Ritter, C. Matschi, D. Schwarz, Assessment of five control strategies of an adjustable glazing at three different climate zones, J. Facade Des. Eng. 3 (2015) 129–141, https://doi.org/10.3233/FDE-130036.

[24] L.L. Fernandes, E.S. Lee, G. Ward, Lighting energy savings potential of split-pane electrochromic windows controlled for daylighting with visual comfort, Energy Build. 61 (2013) 8–20, https://doi.org/10.1016/j.enbuild.2012.10.057.

[25] S. Fathi, A. Kavoosi, Effect of electrochromic windows on energy consumption of high-rise office buildings in different climate regions of Iran, Sol. Energy 223 (2021) 132–149, https://doi.org/10.1016/j.solener.2021.05.021.

[26] F. Isaia, M. Fiorentini, V. Serra, A. Capozzoli, Enhancing energy efficiency and comfort in buildings through model predictive control for dynamic façades with electrochromic glazing, J. Build. Eng. 43 (2021), 102535, https://doi.org/10.1016/j.jobe.2021.102535.

[27] C. Dacquay, H. Fujii, E. Lohrenz, H.M. Holländer, Feasibility of thermal load control from electrochromic windows for ground coupled heat pump optimization, J. Build. Eng. 40 (2021), 102339, https://doi.org/10.1016/j.jobe.2021.102339.

[28] D.-K. Bui, T.N. Nguyen, A. Ghazlan, T.D. Ngo, Biomimetic adaptive electrochromic windows for enhancing building energy efficiency, Appl. Energy 300 (2021), 117341, https://doi.org/10.1016/j.apenergy.2021.117341.

[29] H. Alkhatib, P. Lemarchand, B. Norton, D. O'Sullivan, Optimal temperature actuated control of a thermally insulated roller blind, SSRN Electron. J. (2023), https://doi.org/10.2139/ssrn.4372791.

[30] H.O. Bansal, R. Sharma, P.R. Shreeraman, PID controller tuning techniques: a review, J. Control Eng. Technol. 2 (2012) 168–176. https://www.researchgate.net/publication/316990192_PID_Controller_Tuning_Techniques_A_Review.

[31] V. Singh, V.K. Garg, Tuning of PID controller for speed control of DC motor using soft computing techniques - a review, Int. J. Appl. Eng. Res. 9 (2014) 1141–1147. https://www.ripublication.com/aeee_spl/aeeev4n2spl_05.pdf.

[32] T.M. Kull, M. Thalfeldt, J. Kurnitski, PI parameter influence on underfloor heating energy consumption and setpoint tracking in nZEBs, Energies 13 (2020) 2068, https://doi.org/10.3390/en13082068.

[33] A. Ghoshal, V. John, Anti-windup schemes for proportional integral and proportional resonant controller, in: National Power Electronic Conference, 2015. https://www.researchgate.net/publication/277879787_Anti-windup_Schemes_for_Proportional_Integral_and_Proportional_Resonant_Controller.

[34] Modelica Buildings Library, Buildings Controls Continuous, Buildings Library 8.0.0, 2021. https://simulationresearch.lbl.gov/modelica/releases/v3.0.0/help/Buildings_Controls_Continuous.html#Buildings.Controls.Continuous.LimPID. (Accessed 10 August 2021).

[35] Yudong Ma, F. Borrelli, B. Hencey, B. Coffey, S. Bengea, P. Haves, Model predictive control for the operation of building cooling systems, IEEE Trans. Control Syst. Technol. 20 (2012) 796–803, https://doi.org/10.1109/TCST.2011.2124461.
[36] F. Oldewurtel, A. Parisio, C.N. Jones, D. Gyalistras, M. Gwerder, V. Stauch, B. Lehmann, M. Morari, Use of model predictive control and weather forecasts for energy efficient building climate control, Energy Build. 45 (2012) 15–27, https://doi.org/10.1016/j.enbuild.2011.09.022.
[37] D. Sturzenegger, D. Gyalistras, M. Morari, R.S. Smith, Model predictive climate control of a Swiss office building: implementation, results, and cost–benefit analysis, IEEE Trans. Control Syst. Technol. 24 (2016), https://doi.org/10.1109/TCST.2015.2415411, 1–12.
[38] F. Jorissen, G. Reynders, R. Baetens, D. Picard, D. Saelens, L. Helsen, Implementation and verification of the IDEAS building energy simulation library, J Build Perform Simul 11 (2018) 669–688, https://doi.org/10.1080/19401493.2018.1428361.
[39] C. Aghemo, J. Virgone, G.V. Fracastoro, A. Pellegrino, L. Blaso, J. Savoyat, K. Johannes, Management and monitoring of public buildings through ICT based systems: control rules for energy saving with lighting and HVAC services, Frontiers of Architectural Research 2 (2013) 147–161, https://doi.org/10.1016/j.foar.2012.11.001.
[40] D.H. Blum, N. Xu, L.K. Norford, A novel multi-market optimization problem for commercial heating, ventilation, and air-conditioning systems providing ancillary services using multi-zone inverse comprehensive room transfer functions, Sci Technol Built Environ 22 (2016) 783–797, https://doi.org/10.1080/23744731.2016.1197718.
[41] J. Drgoňa, J. Arroyo, I. Cupeiro Figueroa, D. Blum, K. Arendt, D. Kim, E.P. Ollé, J. Oravec, M. Wetter, D.L. Vrabie, L. Helsen, All you need to know about model predictive control for buildings, Annu. Rev. Control 50 (2020) 190–232, https://doi.org/10.1016/j.arcontrol.2020.09.001.
[42] J. Mäkitalo, Simulating Control Strategies of Electrochromic Windows, 2013. https://www.diva-portal.org/smash/get/diva2:678505/fulltext01.pdf.
[43] M. Jetté, K. Sidney, G. Blümchen, Metabolic equivalents (METS) in exercise testing, exercise prescription, and evaluation of functional capacity, Clin. Cardiol. 13 (1990) 555–565, https://doi.org/10.1002/clc.4960130809.
[44] American Society of Heating Refrigerating and Air-conditioning Engineers, Standard 62.1-2016 – Ventilation for Acceptable Indoor Air Quality, 2019. https://www.techstreet.com/ashrae/standards/ashrae-62-1-2016?product_id=1912838. (Accessed 23 December 2022).
[45] American Society of Heating Refrigerating and Air-conditioning Engineers, Thermal Environmental Conditions for Human Occupancy, 2020. https://www.ashrae.org/technical-resources/bookstore/standard-55-thermal-environmental-conditions-for-human-occupancy.
[46] C. Ticleanu, Lighting in the Workplace – Is it Just about Vision ?, 2019, pp. 1–30. https://iosh.com/media/4142/iosh-2019-cosmin-ticleanu.pdf.
[47] British Standards Institute, BS EN 17037 Daylighting of Buildings, 2018. https://www.bsigroup.com/en-GB/industries-and-sectors/construction-and-building/bs-en-17037-daylighting-of-buildings/. (Accessed 22 December 2022).
[48] A. Ghosh, B. Norton, T.K. Mallick, Daylight characteristics of a polymer dispersed liquid crystal switchable glazing, Sol. Energy Mater. Sol. Cell. 174 (2018) 572–576, https://doi.org/10.1016/j.solmat.2017.09.047.
[49] A. Ghosh, B. Norton, A. Duffy, Daylighting performance and glare calculation of a suspended particle device switchable glazing, Sol. Energy 132 (2016) 114–128, https://doi.org/10.1016/j.solener.2016.02.051.
[50] T. Hong, H. Sun, Y. Chen, S.C. Taylor-Lange, D. Yan, An occupant behavior modeling tool for co-simulation, Energy Build. 117 (2016) 272–281, https://doi.org/10.1016/j.enbuild.2015.10.033.
[51] J.L.M. Hensen, R. Lamberts, Building Performance Simulation for Design and Operation, second ed., Routledge, Abingdon, Oxon, 2019 https://doi.org/10.1201/9780429402296.